ACS Catalysis

Research Article

pubs.acs.org/acscatalysis

Microwave-Assisted Selective Oxidation of 1-Phenyl Ethanol in Water Catalyzed by Metal Nanoparticles Immobilized onto Supported Ionic Liquidlike Phases

Julian Restrepo,[†] Raul Porcar,[†] Pedro Lozano,[‡] M. Isabel Burguete,[†] Eduardo García-Verdugo,*[,†] and Santiago V. Luis*[,†]

[†]Department of Inorganic and Organic Chemistry, University Jaume I, Avenida Sos Baynat s/n, E-12071 Castellón, Spain

[‡]Departamento de Bioquímica y Biología Molecular B e Inmunología, Facultad de Química, Universidad de Murcia, Campus de Espinardo, E-30100 Murcia, Spain

Supporting Information

ABSTRACT: The catalytic activity of metal nanometallic particles (MeNPs) immobilized and stabilized onto supported ionic liquidlike phases is evaluated to develop Au- and Pd-based oxidation catalytic systems. Under similar conditions, AuNPs behave as more active catalysts than PdNPs. In these systems, the polymer support is not only an inert matrix. Indeed, the polymer is designed to play a pivotal role. The polymeric backbone adequately modified with ionic liquidlike moieties (supported ionic liquidlike phases, SILLPs) actively plays several roles, facilitating the stabilization of the metal nanoparticles, controlling the easy accessibility of the reagents/substrates to the active sites, and providing specific microenvironments for an efficient and selective absorption of the microwave electromagnetic irradiation. The structure of these supports can be tuned to adjust the catalytic efficiency of the MeNP−SILLP composites. For this purpose, the Taguchi methods represent, as shown here, a very valuable tool. In the search for more environmentally friendly conditions, the oxidation reactions could be performed by combining microwave heating (as energy source), water (as solvent), and hydrogen peroxide (as a benign oxidant), achieving a more sustainable process.

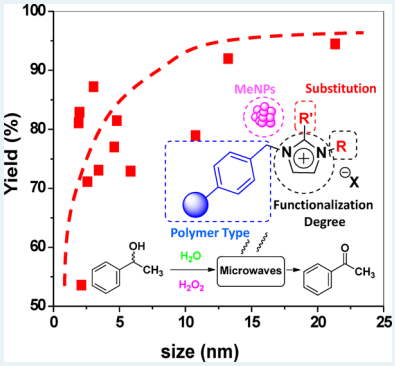

KEYWORDS: *ionic liquid, supported ionic liquid, SILLPs, polymeric ionic liquid, polymer supported catalyst, gold, NPs oxidation, microwave*

1. INTRODUCTION

In the search for greener and advanced chemical processes, the so-called *enabling technologies* have emerged in the past decade and have significantly influenced the way organic synthesis is conducted.[1] In general, enabling technologies can be defined as traditional or new techniques whose purpose is to speed up synthetic transformations and facilitate the workup as well as the isolation of products. Typical enabling technologies can be (i) solid phase assistance, such as the use of hetereogenized reagents or catalysts;[2] (ii) nonclassical or new solvent systems, such as supercritical fluids, perfluorinated solvents or ionic liquids; or (iii) new heating devices, such as microwave (μw) irradiation or inductive heating. Very often, the combination of at least two or more of these enabling technology tools will not only add the inherent advantages of each one considered individually, but will produce a synergistic effect, allowing the development of greener and more efficient chemical processes.

Among these tools, the inherent advantages of catalysis for achieving more efficient, more selective, and less energy-intensive chemical processes is well established.[3] In this context, catalysts based on metal nanoparticles (MeNPs) of noble metals are gaining importance in different synthetic fields.[4−6] In particular, gold nanoparticles (AuNPs) have been used frequently because of their high surface area and size-dependent properties, allowing achievement of efficient processes with high conversions, yields, and selectivities.[7,8] However, the catalytic performance of these nanomaterials strongly relies on the preparation and stabilization techniques employed to avoid aggregation during the different steps of their preparation and application. In this regard, the use of functional polymeric materials can be expected to play an essential role in the entrapping, immobilization, and stabilization of MeNPs.[9] Polymer-supported MeNPs not only stabilize them but also facilitate their separation and reuse.[10,11] However, the support, in many cases, is not a mere inert spectator used for the catalyst heterogenization.[12]The support can play an active role in tuning the catalytic activity.[13] Indeed, the nature of the support can be designed to favor the accessibility of the reagents to the active sites and the further isolation of the products.[14] The appropriate selection of a support has been shown to significantly increase the efficiency of the supported catalyst in terms of activity, selectivity, and stability.[15]

Received: June 1, 2015
Revised: July 2, 2015
Published: July 3, 2015

DOI: 10.1021/acscatal.5b01129
ACS Catal. 2015, 5, 4743−4750

In this context, we have focused our recent research efforts on the development of the so-called supported ionic liquidlike phases (SILLPs) prepared by the immobilization of molecules with IL-like structures onto solid polymeric supports (Scheme 1). These advanced materials allow transferring the ILs properties to the solid phase. Thus, SILLPs share the properties of true ILs and the advantages of a solid polymeric support.[16] Different catalytic processes can be developed based upon the immobilization of a wide range of catalytic moieties onto these SILLPs.[17,18] As for bulk ILs, the presence of the IL-like fragments in SILLPs provide different mechanisms to control the overall efficiency of the catalysts supported on them.[19,20]

Scheme 1. Microwave-Assisted Selective Oxidation of 1-Phenyl Ethanol in Water Catalyzed by AuNPs−SILLP

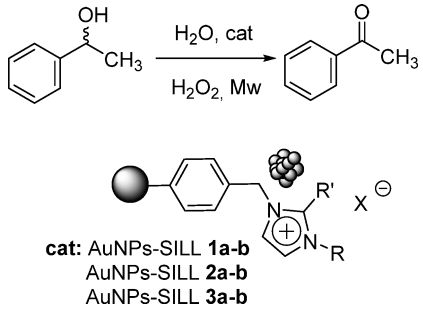

The use of microwave irradiation is another spreading enabling technique in the field of organic chemistry. Microwave irradiation is a cleaner and more efficient energy source than the traditional convective heating.[21] On the other hand, ionic liquids (ILs) are good candidates for microwave heating because of their polar character.[22] Hence, microwave-assisted synthesis using ILs has also been explored to facilitate organic synthesis.[23] The combination of microwave irradiations and catalysts based on MNPs and supported ILs may provide several advantages and possible synergies leading to more efficient catalytic process. This work shows our efforts to combine these enabling technologies in a single process for the oxidation of 1-phenyl-ethanol with H_2O_2 as oxidant. The synergetic combination of these enabling tools greatly enhances catalytic activity in the search for more sustainable oxidation reactions.

2. RESULTS AND DISCUSSION

AuNP−SILLP Synthesis. We have recently developed a simple and fast methodology for the preparation of stable AuNPs immobilized onto SILLPs.[24,25] The aim of this work was to optimize the application of these composites as oxidation catalysts, considering the overall reaction conditions and the composition of the composite, with particular emphasis on the different structural and morphological parameters of the support as key elements. Thus, the efficiency of 12 different AuNP−SILLP composites as catalysts for the oxidation of 1-phenyl-ethanol (**4**) to acetophenone (**5**) using water peroxide (H_2O_2) as a green oxidant has been investigated. SILLPs with different structural variations have been selected to evaluate if the catalytic activity of the resulting AuNPs−SILLPs can be tuned by the nature of the polymeric backbone.

Table 1 gathers the three main structural variations considered regarding the nature of the SILLPs. Thus, SILLPs with different IL-like units and loading (low vs high loadings) were assayed. For the polystyrene backbones considered, the low loadings correspond to having <20% of the aromatic rings from styrene functionalized, whereas for high loadings, this DF increases to more than 20−80%. In this way, the low functionalization degree was selected in the range 12−25% IL-like units by weight, and high loadings are in the range of 37−64%. The polymeric backbone of the cross-linked SILLPs was also varied, and regarding the cross-linking degree, both gel and macroporous resins were used. Finally, different substitution patterns of the imidazolium moiety (R = $-CH_3$ R′ = −H (**1**); R = $-C_4H_9$ R′ = $-CH_3$ (**2**) and R = $-C_{10}H_{21}$ R′ = $-CH_3$ (**3**)) were evaluated. These SILLPs were used for the immobilization of AuNPs according to the methodology previously reported.[24] The morphological properties of these AuNPs−SILLPs, as obtained by DR−UV−vis and TEM analysis, are shown in Table 1. Thus, depending on the SILLP used as the support, AuNPs with narrow size distributions (1.5−23 nm) can be prepared. Both the polymeric framework and the IL-like moieties (type and loading) contribute to the nucleation and stabilization of the gold nanoparticles.[24]

Table 1. Characteristics of the AuNPs−SILLPs Prepared from SILLPs[a]

entry	AuNP−SILLP	R	R′	loading[b]	λ_{max}[c]	TEM[d]
1	**1a** (g)	CH_3	H	3.18 (37)	526	4.73 ± 3.2
2	**1b** (m)	CH_3	H	3.79 (44)	547	13.2 ± 8.3
3	**1c** (g)	CH_3	H	1.01 (12)	525	2.57 ± 0.90
4	**1d** (m)	CH_3	H	1.09 (13)	522	1.97 ± 0.51
5	**2a** (g)	C_4H_9	H	2.80 (45)	530	4.59 ± 1.72
6	**2b** (m)	C_4H_9	H	3.27 (52)	539	10.72 ± 4.79
7	**2c** (g)	C_4H_9	H	0.97 (15)	530	3.41 ± 2.68
8	**2d** (m)	C_4H_9	H	1.04 (17)	545	5.83 ± 3.82
9	**3a** (g)	$C_{10}H_{21}$	CH_3	2.20 (57)	547	21.3 ± 10.0
10	**3b** (m)	$C_{10}H_{21}$	CH_3	2.47 (64)	527	3.02 ± 1.08
11	**3c** (g)	$C_{10}H_{21}$	CH_3	0.88 (23)	528	1.90 ± 0.43
12	**3d** (m)	$C_{10}H_{21}$	CH_3	0.95 (24)	540	2.11 ± 0.94

[a]Gold loading of all AuNPs−SILLPs 0.05 mmol/g; g indicates gel-type, m indicates monolith. [b]mmol/g calculated by elemental analysis; in parentheses, percent by weight of IL-like units. [c]SPR for the AuNPs−SILLPs obtained after reduction. [d]Average size as measured by TEM.

Effect of Solvent, Base, Catalyst Loading and Temperature. The potential and efficiency of the designed AuNP−SILLP composites as active and stable catalysts were investigated in the oxidation of alcohols in water. The oxidation of 1-phenyl ethanol to afford the corresponding ketone was selected as the model reaction. H_2O_2 was used as a clean oxidation agent. The influence of the different experimental factors on the performance of the catalysts was evaluated using a DoE approach based on the Taguchi methods.[26]

The DoE allows determining which experimental factor has a greater influence on the catalytic performance and which ones have less. Thus, the effect of the solvent was first evaluated using different organic solvents (acetonitrile, THF, toluene, and water). The reactions were performed at 125 °C under μw irradiation (50 W working at fixed temperature mode) and for 15 min. The 12 catalysts listed in Table 1 were assayed for this study. The calculated TOF values (mol ketone × mol cat.$^{-1}$ × h^{-1}) are gathered in Table S1. They allowed us to find out the influence of the solvent by plotting the mean TOF value obtained according to the DoE principles versus solvent nature (Figure 1). The results suggest that the catalysts are more

DOI: 10.1021/acscatal.5b01129
ACS Catal. 2015, 5, 4743−4750

efficient when water is used as the reaction media, independently of the nature of the catalyst.

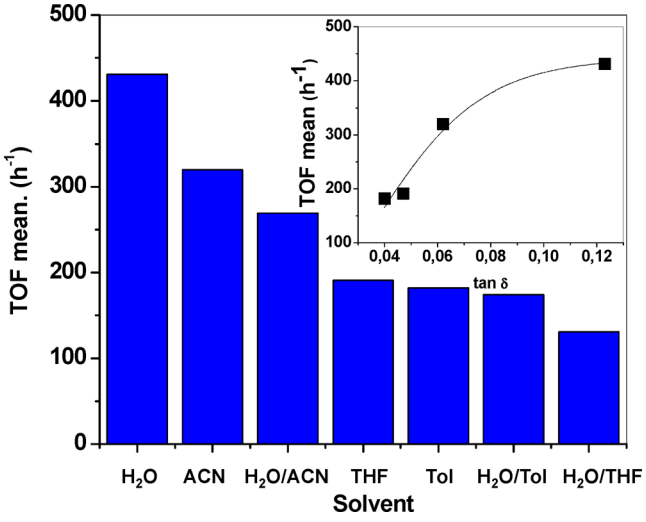

Figure 1. Evaluation of the influence of different solvents on the catalyst efficiency by a DoE based on the Taguchi methods. TOF mean values for the different solvents and solvent mixtures used. Inset: TOF mean value versus solvent loss factor. Conditions: 125 °C; 15 min, microwave irradiation power 50 W; solvent ratio H_2O/H_2O_2 = 1.5/0.5 mL; 0.41 mmol 1-phenyl ethanol; 0.41 mmol, 0.25 mol % cat. AuNP−SILLP (**1a**).

These results are easy to rationalize if the loss factor of each solvent is considered (see inset in Figure 1). The efficiency of the reaction was enhanced with the increase in the loss factor of the solvent used as the medium. Solvents with a higher loss factor are able to transform in a more efficient way the electromagnetic irradiation on reaction heat. Accordingly, H_2O is the most suitable solvent for this reaction in terms of catalyst efficiency, easy workup, and compliance with the green chemistry principles.

Once water was established as the most efficient solvent, the effects of additional experimental factors were also evaluated. Thus, the reaction was performed in water in the absence and presence of different amounts of the AuNP−SILLP **1a** (Figure 2). Although the reaction proceeded slowly in the absence of

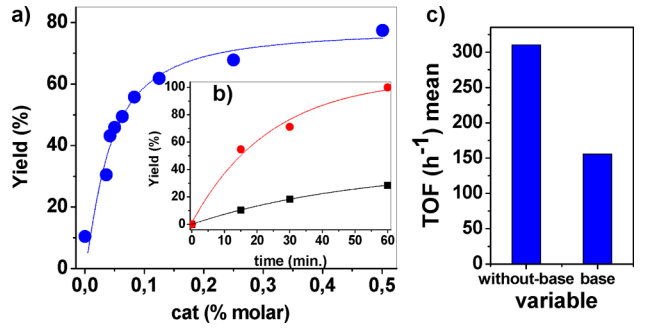

Figure 2. (a) Yield for the oxidation of 1-phenyl ethanol vs the amount of catalyst (AuNP−SILLP **1a**, mol %). (b) Oxidation of 1-phenyl ethanol in the presence or absence of catalyst. ●: catalyzed (**1a**, 0.25 mol %). ■: uncatalyzed. (c) Evaluation of the effect of the base by a DoE method. Conditions: 150 °C; 15 min, microwave irradiation power 50 W; ratio H_2O/H_2O_2 = 1.5/0.5 mL; 0.41 mmol 1-phenyl ethanol; 0.24% mol cat. AuNP−SILLP **1a**.

the catalyst, a clear enhancement of the activity was achieved by the action of the catalyst. Indeed, after 1 h, the presence of **1a** yielded a full conversion of the alcohol to the corresponding ketone, and the uncatalyzed reaction seems to have reached a plateau leading to ∼20% of conversion (Figure 2b). The results also showed that an increase in the molar amount of the AuNPs provided an increase in the catalytic activity (Figure 2a). The activity reached saturation around 0.5 mol % (with respect to alcohol). In consequence, ∼0.25 mol % can be considered as the optimum value leading to good yields with a reasonable low level of catalyst. Finally, using DoE, the effect of the presence/absence of base (KOH) was also studied (see the Supporting Information, Table S2). Our results showed that the catalyst (**1a**) is more efficient in the absence of a base, displaying an almost 2-fold increase in its activity when the base is not present (Figure 2c).

The effect of the temperature was also investigated for the different catalysts prepared. A similar temperature dependence was observed for all of the catalysts assayed (Figure S1). The yield increased significantly (yield > 40%) for higher temperatures (>120 °C). This yield enhancement showed a clear exponential increase with the temperature according to the Arrhenius's law. Thus, the use of these data allows calculating the frequency factor (A) and the activation energy (E_a) for the different catalysts tested (Table S3). Altogether, the results put forward that the optimized conditions for the H_2O_2 oxidation of 1-phenyl ethanol involve using 0.25 mol % of catalyst, water as the solvent, an absence of added inorganic bases, and microwave irradiation at 150 °C.

Effect of the AuNP−SILLP Composition, Structure and Morphology on the Catalytic Efficiency. Once the optimal experimental conditions were identified, the influence of the structure and morphology of the polymeric SILLPs to tune the catalytic efficiency of the supported AuNPs was evaluated. We have recently demonstrated that the appropriate selection of the structural parameters of the polymeric SILLPs, such as resin morphology and the loading and nature of the IL-like groups, can influence not only the size distribution of the metal nanoparticles but also the catalytic activity of different species immobilized onto the SILLPs.[16−18,20] Furthermore, the presence of the IL-like units can also influence how the microwave irradiation is absorbed and transformed into heat in a way similar to that reported for bulk ILs.[16] To evaluate such effects, we decided to carry out the 1-phenyl ethanol oxidation reaction at two different temperatures (100 and 150 °C), several reaction times (15, 30, 60, and 120 min), and using the 12 catalysts prepared. The results obtained are gathered in Figures S3, S4. The adjustment of these data to a first-order reaction kinetic permitted us to calculate the reaction rates for the different catalysts (Tables S4−7). The use of DoE provides a simple method to simultaneously evaluate the effect of the nature of the polymeric SILLPs on the reaction rates and therefore on the catalysts' efficiency. Variables include the functionalization degree (low vs high; i.e., 12−25% IL-like weight vs 37−64%), resin morphology (gel type vs macroporous), and the alkyl substitution of the imidazolium moiety (methyl (Me-), butyl (But-), or decyl (Dec-)). The effect of these variables can be analyzed (considering a DoE approach) by plotting the mean reaction rate constant and the mean gold particle sizes against the different levels of the variables considered. Figure 3 depicts the trends found for the different variables studied on the basis of evaluation of the 12 catalysts.

DOI: 10.1021/acscatal.5b01129
ACS Catal. 2015, 5, 4743−4750

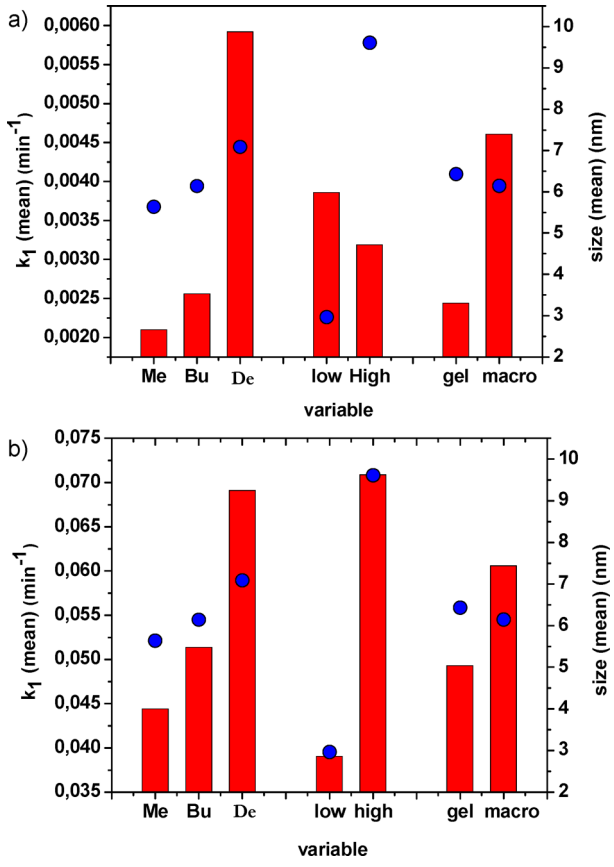

Figure 3. Effect of different variables on the mean reaction rate, by DoE analysis, for the oxidation of 1-phenyl ethanol: (a) 100 °C and (b) 150 °C. μw power = 50 W, H_2O/H_2O_2 = 1.5/0.5 mL. Bar: mean reaction rate constant (min^{-1}). Dots: AuNPs' mean size distribution (nm).

The figure also includes a similar analysis of how the AuNP size distribution is affected by the same variables.

It is to be noted that the larger the mean reaction rate constant for a given parameter, the more influence this particular variable displays over the catalyst efficiency. Thus, the results suggest that at 100 °C, the alkyl chain length was the variable providing a larger effect, and the effect of the IL-like units loading was the least pronounced. Regarding the criteria "larger, more efficient", the DoE analysis at 100 °C indicated that the more efficient catalyst can be obtained by using macroporous AuNP−SILLPs with low loading imidazolium units bearing as the N-substituent a long alkyl chain (Dec-); however, at 150 °C, the variable displaying a larger influence was the loading of IL-like units, followed by the imidazolium substitution pattern. In this case, the most efficient system can be obtained on the same basis as the combination at 100 °C but using highly loaded SILLPs. In most cases, there is a close relationship between the most influential variable and the AuNPs' mean size distribution.

Summarizing these results, the DoE analysis suggests that an increase in the chain length on the imidazolium, following the order meth-, but-, and dec- leads to an enhancement of the reaction rate. This trend also matches the one observed for AuNP size distribution, because the longer the alkyl chain, the bigger the AuNP size distribution. There is also a clear relationship between the type of resin used and the reaction rate; hence, the larger reaction rates are found for AuNP−SILLPs based on macroporous resins.

These results clearly indicate the noninnocent role of the support in the catalytic behavior of the AuNPs. Thus, for instance, the better performance of the macroporous resins in comparison with the gel-type resins can be rationalized attending to different elements. It is well-known that very often, the efficiency of catalysts immobilized onto macroporous resins is related to the facilitated diffusion of the reagents to the active sites through the permanent porosity of these materials.[27] The diffusion is affected by the support wettability, understanding by wettability we mean the compatibility and/or the affinity of the support for the reaction medium, reagents, and products (i.e., hydrophilicity, and hydrophobicity).[14] A polymeric support with adequate wettability will favor the diffusion of the reactants and product to or from the active sites affecting the catalytic efficiency. The modification of the polymer matrix with ionic liquidlike units induces a change in its polarity, shifting the hydrophobic PS-DVB matrix into a hydrophilic material, enabling water diffusion. Figure 4 clearly illustrates this phenomenon. The

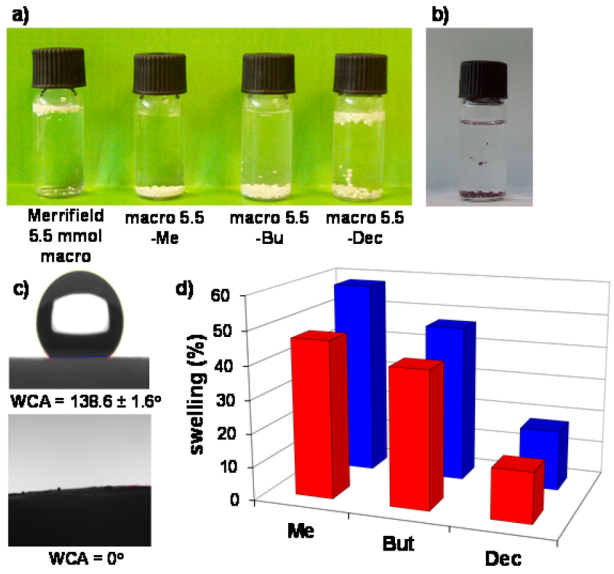

Figure 4. Water compatibility for AuNPs−SILLPs. (a) Behavior of SILLPs resins in water. (b) Behavior of AuNPs−SILLP **1b** in water. (c) Water contact angle: Merrifield resin, 5.5 mmol Cl/g (left); AuNPs−SILLPs **1b** (right). (d) Percent swelling for AuNP−SILLPs (blue): Me (**1a**), But (**2a**), and Dec (**3a**) and related SILLPs precursors (red).

unmodified Merrifield macroporous resins are not wet by water (water contact angle (WCA) = 138 °) floating on the top of the vial, whereas water can be absorbed onto SILLPs having chloride as the anion. Consequently, water filled the porous of the polymer, and the SILLP sank to the bottom of the vial (WCA = 0°). The length of the alkyl chain can be used to fine-tune the hydrophobicity/hydrophilicity balance of the IL-like microenvironment, and recent studies have shown that SILLP polymers can act as potent sorbents for organic compounds used in solid-phased extractions.[28,29] Indeed, the use of long alkyl chains (Dec-) provided SILLPs with some degree of amphiphilic behavior, with SILLP particles located both at the top and at the bottom in water. In our case, these long alkyl chains (Dec-) can favor the absorption of the substrate in

DOI: 10.1021/acscatal.5b01129
ACS Catal. 2015, 5, 4743−4750

comparison with SILLPs bearing shorter alkyl chains. The consequence should be a higher local concentration within the pores of the polymer and an enhanced catalytic efficiency of the AuNPs embedded in the IL-like microenvironment through this favorable substrate concentration gradient. A similar behavior is observed for SILLPs and AuNP−SILLPs in this regard (Figure 4b).

On the other hand, gel-type resins, having only 2% cross-linking, require the swelling of the polymeric matrix to fully expose the catalytic sites. The unmodified Merrifield resin, being a hydrophobic polymer, shrinks in water, whereas all the SILLPs showed an appreciable swelling in water, even when the imidazolium is substituted with long alkyl chains. As a matter of fact, the swelling in water can be tuned by changing the length of the alkyl chain of the imidazolium moieties (Figure 4d). The presence of gold nanoparticles also seems to contribute to the swelling of the AuNP−SILLP gel-type composites. Indeed, the AuNPs−SILLPs showed a slightly larger swelling than the corresponding SILLP supports (i.e., **1a** 58% vs 47%; **2a** 47% vs 41%; **3a** 18% vs 15%, Figure 4d and Figure S5).

In the case of get-type resins, an appropriate swelling will decrease the diffusional limitations usually associated with these materials, but not completely, which should explain the reduced activity of the corresponding catalysts in comparison with the macroporous ones. On the other hand, the presence of long aliphatic chains (decyl) can contribute again to preconcentrate the substrates in the proximity of the catalytic centers, in particular for high loadings of the imidazolium subunits, as suggested experimentally by the high relative activity detected for **3a** and **3b** at 150 °C.

Finally, it is important to note that the variation of the structural features of the SILLPs also affects the sizes of the AuNPs obtained.[24] The DoE analysis (Figure 3) seems to indicate that in many cases, there is an enhancement of the catalytic efficiency with the increase on the AuNP sizes.

To confirm this effect, the yields obtained for all the catalysts evaluated were plotted against the corresponding AuNP sizes (Figure 5). In general, the yield increased with the AuNP sizes,

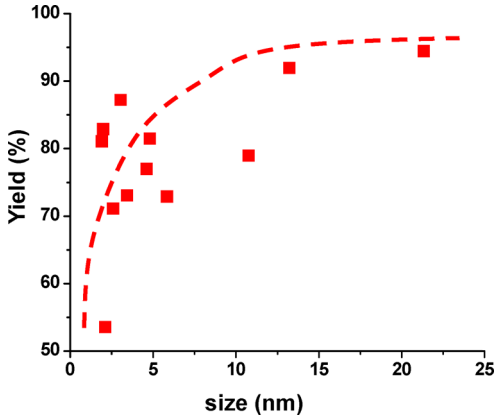

Figure 5. Yield (%) vs AuNP size (nm). 150 °C. μw power = 50 W; H_2O/H_2O_2 = 1.5/0.5 mL; 0.24% mol cat.

reaching a plateau around 15−20 nm. Because the particle size is not the only factor contributing to the catalytic efficiency of these composites, a clear deviation from the general trend is observed for some catalysts. In general, higher catalytic activities use to be associated with the smaller MeNPs. In this case, the opposite effect is observed, and one possible explanation could be related to the formation of "hot-spots" on the NPs through an efficient absorption of the microwave irradiation. The heat transfer from the NP to the environment is proportional to the surface area where the heat exchange occurs.[30,31] Thus, for bigger AuNPs, an appreciable temperature gradient can be established between particle and bulk liquid.

However, when the catalytic behavior of two AuNPs stabilized with citrate (average particle sizes of 6 and 9 nm) were tested in solution, under the same experimental conditions in the absence of any SILLP, the yields obtained for the ketone were 100% and 54%, respectively. Thus, in the absence of the support, an inverse relationship between the AuNP size and activity was observed: the smaller the AuNP size, the greater the catalytic activity. These results highlight that the enhancement of the catalytic efficiency for SILLPs containing larger AuNPs must also involve an important participation of the support, including the IL fragments attached to the polymeric backbone. As a matter of fact, ILs are excellent media for microwave heating because of their polar character. We have demonstrated that SILLPs share the main features of the bulk ILs regarding their heating under microwave irradiation.[16,32] Indeed, SILLPs are advanced polymeric materials with well-defined IL-like domains able to efficiently absorb microwave irradiation. Figure 6 depicts the

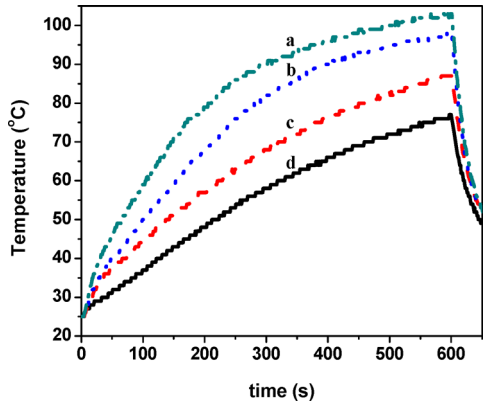

Figure 6. Microwave heating profiles (temperature (°C) vs time) for different systems. (a) AuNP−SILLP **1a**; (b) SILLP precursor for **1a**; (c) Merrifield resin, 4.3 mequiv/g, 2% DVB; (d) in the absence of polymer. Conditions: benzene vol = 2 mL, polymer = 20 mg, μw (power constant = 50 W), time = 10 min.

heating profiles obtained in a solvent transparent to the microwave irradiation (benzene) alone and in the presence of a Merrifield resin, the AuNP−SILLP (**1a**) and its immediate SILLP precursor using a constant μw power.

The efficiency of the heating follows the trend: absence of support (76 °C) < Merrifield resin (87 °C) < SILLP (97 °C) < AuNP−SILLP (**1a**) (102 °C). Both AuNPs and SILLPs contribute to enhancement of the solvent heating by transferring to it the microwave irradiation absorbed. Therefore, both AuNPs and SILLPs can act synergistically to improve the efficiency of the reaction by absorbing the electromagnetic irradiation onto the IL-like heated microdomains of SILLPs, inducing a "selective-heating" of the AuNPs present in the IL-like domain. This effect can be more efficient for larger AuNPs, creating higher local temperatures and improving the catalytic activity.

DOI: 10.1021/acscatal.5b01129
ACS Catal. 2015, 5, 4743−4750

Oxidation with PdNPs−SILLPs and Mixed Metal Pd−AuNP−SILLP. The synthesis of PdNPs−SILLPs can also be easily performed by the initial adsorption onto the SILLPs of the $PdCl_4^-$ metal precursor and its further reduction with $NaBH_4$.[17,33] Table 2 gathers the main characteristics of the

Table 2. Characteristics of the PdNPs−SILLPs Prepared from SILLPs

entry	R	IL loading LI (mmol/g)[c]	PdNP−SILLP	Pd loading (mmol/g)	size[d] (nm)	yield (%)[e]
1	CH_3[a]	3.03	**4a**	0.95	4.7	92
2	CH_3[a]	3.03	**4b**	1.94	57.3	92
3	C_4H_9[a]	2.64	**4c**	0.95	12.2	87
4	CH_3[a]	0.64	**4d**	0.95	4.4	63
5	CH_3[b]	1.27	**4e**	0.95	6.1	49
6	C_4H_9[b]	1.12	**4f**	0.95	11.2	96

[a]Gel-type. [b]Macroporous. [c]Calculated by elemental analysis. [d]TEM. [e]Yield for the oxidation of 1-phenyl ethanol. Conditions: temp = 150 °C, 15 min, low stirring, μw = 50 W, H_2O/H_2O_2 = 1.5/0.5 mL, 0.24% mol cat.

SILLPs and the corresponding PdNPs−SILLPs obtained from them. The obtained PdNPs loadings were larger than those for the related gold composites. The sizes of the resulting PdNPs were in the range of 4−15 nm. Only in the case of very high palladium loadings were larger nanoclusters observed (entry 2, Table 2). The different PdNPs−SILLPs were also tested as catalysts in the same oxidation model reaction. The PdNPs composites were shown to be active catalysts for the oxidation of 1-phenyl-ethanol, with yields ranging from 40 to 96%. When the yields for the different catalysts were plotted against the PdNPs size, a trend similar to that of the one obtained for the AuNPs was found (Figure 7). The catalytic efficiency increased with the PdNPs size until reaching a plateau for particles larger than 10 nm.

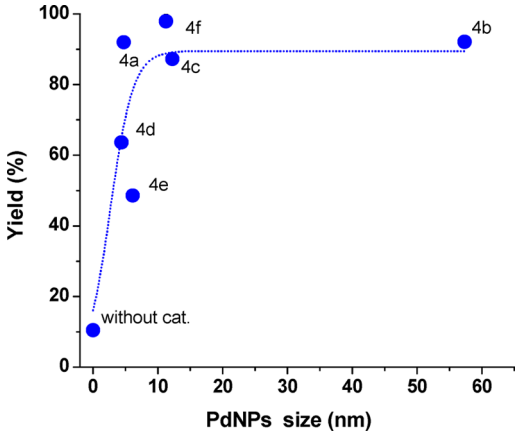

Figure 7. Yield (%) vs PdNPs size (nm). 150 °C. μw power = 50 W, H_2O/H_2O_2 = 1.5/0.5 mL, 0.24% mol cat.

Two additional composites with the same characteristics as AuNP−SILLP **2d** were prepared by substituting the gold with palladium (**5**) and with an equimolecular mixture of gold and palladium (**6**). Both systems led to the corresponding immobilized nanoparticles. The mean size found for the palladium particles for the PdNPs−SILLP (**5**) was significantly larger than those found for the ones containing only gold (**2d**) and a gold−palladium mixture (**6**) (Table 3). These MeNPs−SILLPs were assayed as catalysts for the oxidation. The catalyst

Table 3. Characteristics of the MeNPs−SILLPs Related to AuNP−SILLP 2d

entry	MeNP−SILLP[a]	metal[b]	size[d] (nm)	yield[e]
1	**2d**	Au	5.8 ± 3.8	68
2	**5**	Pd	22.8 ± 15.8	34
3	**6**	Au/Pd[c]	2.9 ± 1.4	100

[a]Macroporous, low loading, But. [b]Compounds **5** and **6** obtained in manner analogous to that for **2d**, metal precursor $PdCl_4^-$ and $AuCl_4^-$; metal loading 0.0507 mmol/g. [c]SILLP was loaded first with $PdCl_4^-$ (0.02535 mmol/g) and then with $AuCl_4^-$ (0.02535 mmol/g) prior to reduction with $NaBH_4$. [d]TEM. [e]Yield for the oxidation of 1-phenyl ethanol. Conditions: temp = 150 °C, 15 min, low stirring, μw = 50 W, H_2O/H_2O_2 = 1.5/0.5 mL, 0.25% mol cat.

based on PdNPs was clearly less efficient than those containing gold. Interestingly, the best catalytic behavior was provided by the composite containing an equimolecular mixture of Pd and Au. This result is in good agreement with previous findings, where the addition of Pd to Au catalysts showed a synergetic increase in both selectivity and activity.[34,35]

Recycling of the AuNPs−SILLPs. Finally, the reusability of the SILLP-supported AuNPs was evaluated using AuNP−SILLP **3b**. The results were disappointing because the catalytic activity decreased for consecutive uses from 67% to 39%, 37%, and 35% for the second to fourth cycles. The aggregation of Me NPs is one of the most common mechanisms for deactivation of their catalytic activity; however, when the DR−UV−visible spectrum of the AuNP−SILLP **3b** was analyzed before and after the reaction, no significant differences were observed (Figure S6), although the TEM analysis revealed an increase in the average particle size from 3.03 to 11.6 nm (see the Supprting Information). This increase in the particle size does not justify the catalyst deactivation. Indeed, and according with the effect observed for the nanoparticle size on the catalytic activity, the change observed could even lead to an enhancement of the catalytic efficiency after the first cycle. A second alternative for deactivation in this kind of systems is the lixiviation of gold during the reaction. In the case of Pd-catalyzed C−C bond forming reactions involving PdNPs−SILLPs, soluble active Pd catalytic species are released from the support, but the SILLPs act as efficient scavengers for these lixiviated metal species, stabilizing them and avoiding the formation of inactive Pd clusters.[17,33] Taking this into account, the model reaction was performed under standard conditions for 15 min, and then the catalyst was filtered off. The same SILLPs used in the preparation of the AuNPs−SILLPs was then added to the resulting solution as a scavenger of the potential metallic nanoclusters present. After stirring the suspension and filtering, washing, and drying the polymers, they were used as catalysts for the model reaction under standard conditions. Table 4 gathers the results obtained for AuNP−SILLPs **1a**, **1b**, and **3b**. In all the cases, an appreciable catalytic activity was observed that is directly related to that of the original AuNPs−SILLPs used, confirming the presence of lixiviated gold species that are efficiently captured by the corresponding SILLPs. Thus, gold lixiviation from the catalytic composite seems to be at the origin of the reduction of the activity observed under recycling.

DOI: 10.1021/acscatal.5b01129
ACS Catal. 2015, 5, 4743−4750

Table 4. Reactions Catalyzed by the SILLPs Used As Scavengers of the Possible Gold Lixiviated Species

entry	AuNP–SILLP	SILLP "scavenger"	description	AuNP–SILLP yield (%)[a]	Au-scavenger composites yield (%)[b]
1	**1a**	**5a**	g-4.3, Me, Cl^-	55	47
2	**1b**	**5b**	m-5.5-Me, Cl^-	68	62
3	**3b**	**7b**	m-5.5-De, Cl^-	67	60

[a]First cycle yield for the initial AuNP–SILLP. [b]Yield obtained with SILLPs **5a**, **5b**, and **7b** after scavenging the Au species lixiviated by the corresponding AuNP–SILLPs in the first cycle.

In light of these and previous results, we decided to evaluate the use of a polymer cocktail to improve the applicability of these catalytic systems.[33] As previously studied, such a cocktail must contain the initial catalytic composite (AuNP–SILLP) along with a basic SILLP (*m*-SILLP 7, X = OH^-, macro, 3.45 mmol OH^-/g), which is expected to act simultaneously as a scavenger for the lixiviated species and as a base to modify the catalytic process. In the first assay, the cocktail was formed by a 20:10 (**3b**:7) weight mixture, and the result was a decrease in the yield for the first cycle (57% yield), although the activity was maintained for the second one (55%). Unfortunately, further reuses showed a significantly reduced catalytic efficiency (24% for third reuse and 20% for the fourth). However, when the amount of the polymeric base on the cocktail was increased (10:50 (**3b**:7) mixture by weight), a positive effect was observed. The yield in the first cycle increased in comparison with the reaction performed in the absence of 7 (82% vs 67%), and the catalytic activity decreased to a lower extent (73% for the second, 58% for the third, and 45% for the fourth use) (Figure 8).

3. CONCLUSIONS

In summary, the present study demonstrates that AuNP–SILLPs composites are able to efficiently catalyze the oxidation of 1-phenyl ethanol in water using H_2O_2 as the oxidant and microwave irradiation as the heat source. The results presented clearly highlight how the efficiency of the catalyst can be tuned by an adequate design of the corresponding SILLPs. Thus, the SILLP support is not a mere spectator and, indeed, plays an active role in the catalytic cycle. The structure and morphology of the SILLPs used as supports may contribute to the stabilization of the nanoparticles determining their size, and therefore their intrinsic activity, but also to regulate the diffusion of the reagents and products to and from the active sites and, finally, to provide the appropriate microenvironment for an efficient and selective absorption of the microwave electromagnetic irradiation. The use of DoE with the application of the Taguchi methods has allowed stressing the relative relevance of the different structural and morphological elements of the SILLPs for the overall catalytic behavior. The combination of microwave irradiation and catalysts based on MeNPs and supported ILs affords important advantages and synergies for the development of more efficient and sustainable catalytic processes, that is, in the field of oxidation reactions as presented here. As with many other examples involving the catalytic application of MeNPs, the lixiviation of the active metal species from the stabilized NPs represents an important mechanism of deactivation that limits the range of their potential applications.; however, the initial results obtained with the use of polymeric cocktails not only reveal their potential to implement the catalytic activity of the systems under study but also open the way to obtain more stable catalytic systems in which efficient release and catch cycles for the active lixiviated metal species can be established and regulated by the exact structure of the functional polymers participating in the cocktail.

A comparison of the results obtained with Au and PdNPs indicates that AuNPs are more efficient for the oxidation process considered under similar conditions. Very interestingly, the preliminary results here presented on AuPdNPs suggest that these kinds of MeNPs are very active catalysts in this regard and are promising candidates for further studies.

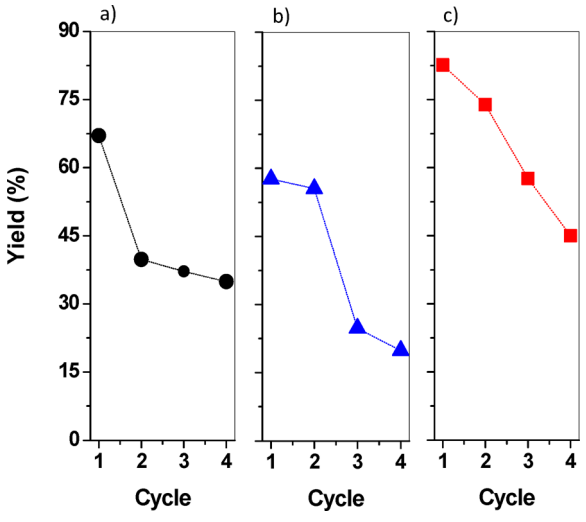

Figure 8. Yields obtained for the reuse of AuNP–SILLPs. (a) **3b**; (b) **3b**/7 (20:10 by weight) and (c) **3b**/7 (10:50 by weight). Conditions: 150 °C, μw power = 50 W, H_2O/H_2O_2 = 1.5/0.5 mL, 0.24% mol cat.

4. EXPERIMENTAL DETAILS

4.1. Materials. All reagents were obtained from Sigma-Aldrich and used without further purification. Gas chromatography (GC) analyses were carried out in a Varian 3900 using a CyclodexB column (length 30m, i.d. 0.25 mm, film 0.25 μm). The microwave irradiation experiments were performed with a Discover System model 908010 from CEM Corporation using custom-made high-purity quartz vials (capacity 10 mL).

The initial SILLPs prepared were analyzed through IR and Raman spectroscopy (for further information, see refs 36–38).

4.2. General Procedure for the Synthesis of MeNPs–SILLPs. The gold AuNPs–SILLPs were synthesized as already reported by us.[24] In brief, the corresponding SILLP was suspended in deionized water, and an aqueous solution of $MeCl_4^-$ was added. The suspension was stirred for 2 h at room temperature. The polymer was then filtered and washed. Finally, the polymer was vacuum-dried at 60 °C. The dry SILLP resin with $MeCl_4^-$ adsorbed was suspended in water, and a solution of $NaBH_4$ was added. The suspension was stirred for 2 h at room temperature for completion of the reduction. Afterward, the polymer was filtered and washed with deionized water and MeOH. Finally, the polymer was dried under vacuum. The obtained AuNPs–SILLPs displayed a red-brown color, indicating the formation of gold nanoparticles. Samples

DOI: 10.1021/acscatal.5b01129
ACS Catal. 2015, 5, 4743–4750

were analyzed and characterized by DR−UV−vis, TEM, and XRD.

4.3. General Procedure for the Oxidation Reaction. The AuNP−SILLP-supported catalyst (20 mg, 0.005 mmol Au/g), 1-phenyl ethanol (50 μL, 0.41 mmol), hydrogen peroxide (0.5 mL, 5.71 mmol), and deionized water (1.5 mL) were introduced into a reinforced glass tube of 10 mL of capacity. The resultant mixture was heated in a microwave oven (CEM Discover, CEM Microwave Technology Ltd., Matthews, NC, USA) at 150 °C with low stirring and 100 Ws. The system was run at constant temperature operation mode by using the air cooling feature of the apparatus and held at this temperature for 15, 30, 60, and 120 min according the experiment. Then the tube was cooled to room temperature. The reaction mixture was extracted with HPLC grade dichloromethane (3 × 7.5 mL), from which 10 mL were taken and analyzed by GC after addition of 1 mL of acetonitrile containing 10 μL of butyl-butyrate as internal standard. All the experiments were carried out in duplicate.

■ ASSOCIATED CONTENT

Supporting Information

The Supporting Information is available free of charge on the ACS Publications website at DOI: 10.1021/acscatal.5b01129.

Details of experimental procedures and characterization results (PDF)

■ AUTHOR INFORMATION

Corresponding Authors

*E-mail: cepeda@uji.es.

*E-mail: luiss@uji.es.

Notes

The authors declare no competing financial interest.

■ ACKNOWLEDGMENTS

This work was supported in part by MINECO, Spain (ref: CTQ2011-28903) Generalitat Valenciana (PROMETEO/2012/020), and UJI-P1-1B2013-37 grants. Cooperation of the SCIC of the UJI for instrumental analyses is acknowledged.

■ REFERENCES

(1) Kirschning, A.; Solodenko, W.; Mennecke, K. *Chem. - Eur. J.* **2006**, *12*, 5972−5990.

(2) Lu, J.; Toy, P. H. *Chem. Rev.* **2009**, *109*, 815−838.

(3) Sheldon, R. A.; Arends, I.; Hanefeld, U. *Green Chemistry and Catalysis*; Wiley-VCH: Weinheim, 2007.

(4) White, R. J.; Luque, R.; Budarin, V. L.; Clark, J. H.; Macquarrie, D.J. *Chem. Soc. Rev.* **2009**, *38*, 481−494.

(5) Astruc, D.; Lu, F.; Aranzaes, J. R. *Angew. Chem., Int. Ed.* **2005**, *44*, 7852−7872.

(6) Yasukawa, T.; Miyamura, H.; Kobayashi, S. *Chem. Soc. Rev.* **2014**, *43*, 1450−1461.

(7) Takale, B. S.; Bao, M.; Yamamoto, Y. *Org. Biomol. Chem.* **2014**, *12*, 2005−2027.

(8) Stratakis, M.; Garcia, H. *Chem. Rev.* **2012**, *112*, 4469−4506.

(9) Kralik, M.; Biffis, A. *J. Mol. Catal. A: Chem.* **2001**, *177*, 113−138.

(10) Biffis, A.; Orlandi, N.; Corain, B. *Adv. Mater.* **2003**, *15*, 1551−1555.

(11) Corain, B.; Jerabek, K.; Centomo, P.; Canton, P. *Angew. Chem., Int. Ed.* **2004**, *43*, 959−959.

(12) Dioos, B. M. L.; Vankelecom, I. F.J.; Jacobs, P. *Adv. Synth. Catal.* **2006**, *348*, 1413−1446.

(13) Madhavan, N.; Jones, C. W.; Weck, M. *Acc. Chem. Res.* **2008**, *41*, 1153−1165.

(14) Wang, L.; Xiao, F. S. *ChemCatChem* **2014**, *6*, 3048−3052.

(15) Altava, B.; Burguete, M. I.; Garcia-Verdugo, E.; Luis, S. V.; Vicent, M. J.; Mayoral, J. A. *React. Funct. Polym.* **2001**, *48*, 25−35.

(16) Sans, V.; Karbass, N.; Burguete, M. I.; Compañ, V.; Garcia-Verdugo, E.; Luis, S. V.; Pawlak, M. *Chem. - Eur. J.* **2011**, *17*, 1894−1906.

(17) Burguete, M. I.; García-Verdugo, E.; Garcia-Villar, I.; Gelat, F.; Licence, P.; Luis, S. V.; Sans, V. *J. Catal.* **2010**, *269*, 150−160.

(18) Lozano, P.; García-Verdugo, E.; Bernal, J. M.; Izquierdo, D. F.; Burguete, M. I.; Sanchez-Gomez, G.; Luis, S. V. *ChemSusChem* **2012**, *5*, 790−798.

(19) Martín, S.; Porcar, R.; Peris, E.; Burguete, M. I.; Garcia-Verdugo, E.; Luis, S. V. *Green Chem.* **2014**, *16*, 1639−1647.

(20) Lozano, P.; García-Verdugo, E.; Karbass, N.; Montague, K.; De Diego, T.; Burguete, M. I.; Luis, S. V. *Green Chem.* **2010**, *12*, 1803−1810.

(21) de la Hoz, A.; Loupy, A. *Microwaves in Organic Synthesis*; Wiley-VCH: Weinheim, 2012.

(22) Hoffmann, J.; Nuchter, M.; Ondruschka, B.; Wasserscheid, P. *Green Chem.* **2003**, *5*, 296−299.

(23) Martínez-Palou, R. *Mol. Diversity* **2010**, *14*, 3−25.

(24) Burguete, M. I.; Garcıa-Verdugo, E.; Luis, S. V.; Restrepo, J. A. *Phys. Chem. Chem. Phys.* **2011**, *13*, 14831−14831.

(25) Restrepo, J.; Lozano, P.; Burguete, M. I.; García-Verdugo, E.; Luis, S. V. *Catal. Today* **2015** 10.1016/j.cattod.2014.12.023.

(26) Roy, R. *A Primer on the Taguchi Method, Society of Manufacturing Engineers*, EEUU, 1990.

(27) Corain, B.; Zecca, M.; Jerabek, K. *J. Mol. Catal. A: Chem.* **2001**, *177*, 3−20.

(28) Fontanals, N.; Ronka, S.; Borrull, F.; Trochimczuk, A. W.; Marcé, R. M. *Talanta* **2009**, *80*, 250−256.

(29) Fontanals, N.; Borrull, F.; Marcé, R. M. *TrAC, Trends Anal. Chem.* **2012**, *41*, 15−26.

(30) Mennecke, K.; Cecilia, R.; Glasnov, T. N.; Gruhl, S.; Vogt, C.; Feldhoff, A.; Larrubia Vargas, M. A.; Kappe, C. O.; Kunz, U.; Kirschning, A. *Adv. Synth. Catal.* **2008**, *350*, 717−730.

(31) Horikoshi, S.; Serpone, N. *Catal. Sci. Technol.* **2014**, *4*, 1197−1210.

(32) Izquierdo, D. F.; Bernal, J. M.; Burguete, M. I.; Garcıa-Verdugo, E.; Lozano, P.; Luis, S. V. *RSC Adv.* **2013**, *3*, 13123−13126.

(33) Sans, V.; Gelat, F.; Karbass, N.; Burguete, M. I.; Garcia-Verdugo, E.; Luis, S. V. *Adv. Synth. Catal.* **2010**, *352*, 3013−3021.

(34) Enache, D. I.; Edwards, J. K.; Landon, P.; Solsona-Espriu, B.; Carley, A. F.; Herzing, A. A.; Watanabe, M.; Kiely, C. J.; Knight, D. W.; Hutchings, G. J. *Science* **2006**, *311*, 362−365.

(35) Burato, C.; Centomo, P.; Pace, G.; Favaro, M.; Prati, L.; Corain, B. *J. Mol. Catal. A: Chem.* **2005**, *238*, 26−34.

(36) Karbass, N.; Sans, V.; García-Verdugo, E.; Burguete, M. I.; Luis, S. V. *Chem. Commun.* **2006**, *29*, 3095−3097.

(37) Lozano, P.; Garcia-Verdugo, E.; Piamtongkam, R.; Karbass, N.; De Diego, T.; Burguete, M. I.; Luis, S. V.; Iborra, J. L. *Adv. Synth. Catal.* **2007**, *349*, 1077−1084.

(38) Burguete, M. I.; Erythropel, H.; García-Verdugo, E.; Luis, S. V.; Sans, V. *Green Chem.* **2008**, *10*, 401−407.

DOI: 10.1021/acscatal.5b01129
ACS Catal. 2015, 5, 4743−4750